JOURNAL OF JICIVILTECH
INNOVATIONS IN CIVIL ENGINNERING AND TECHNOLOGY

*Article Info*
Received: 28.02.2026
Accepted: 21.05.2026

**Research Article**
*e-ISSN 2687-2129*
*jiciviltech*, ***2026***, *8(1), 1-13*

# Impact of the Code-Based Near-Fault Factor on Buried Steel Pipelines via the Design Response Spectrum: Seydişehir–Ermenek Case Study

*[1]Mustafa KOÇER

[1]*Konya Technical University, Faculty of Engineering, Department of Civil Engineering, Konya, Türkiye, mkocer@ktun.edu.tr, ORCID ID: http://orcid.org/0000-0002-5505-2065*

**Highlights**

- Near-fault effects were quantified using code-based response spectrum and shell FE analysis.
- The near-fault factor increased displacement by 41% and axial strain by about 30%.
- Code-based near-fault effects should be included in seismic design of buried steel pipelines.

**Abstract**

This study investigates the influence of the code-based near-fault factor on the seismic response of buried steel natural-gas pipelines through the design response spectrum approach prescribed in the Turkish Seismic Code for Pipeline Systems and Liquid Storage Tanks (2023). The novelty lies in explicitly incorporating both the maximum-direction and near-fault factors into a spectrum-based finite element assessment and quantitatively evaluating their effects on displacement- and stress-based seismic demands. A planned pipeline route between Seydişehir (Konya) and Ermenek (Karaman), Türkiye, was selected as a case study, and seismic hazard parameters were obtained from the Turkish Seismic Hazard Map. The pipeline was modeled using four-node shell elements, while soil–pipe interaction was represented by linear elastic Winkler springs. Response-spectrum analyses were performed for DD-1, DD-1a, DD-2, and DD-3 ground-motion levels. For the DD-1 level including the near-fault factor, the maximum vertical displacement reached 10.42 mm, and the maximum axial membrane stress was approximately 62 MPa. The inclusion of the near-fault factor increased the maximum vertical displacement by 41% and raised the axial strain and membrane force demands by about 30%. The results demonstrate that neglecting this factor may lead to unconservative estimates of deformation demands in buried steel pipelines near active faults.

***Keywords*** *Buried Steel Pipeline, Near-Fault Factor, Response Spectrum, Soil–Pipe Interaction, Finite Element Model*

*[1]Corresponding author

*To cite this article*
Koçer, M. (2026). Impact of the Code-Based Near-Fault Factor on Buried Steel Pipelines via the Design Response Spectrum: Seydişehir–Ermenek Case Study. Journal of Innovations in Civil Engineering and Technology (JICIVILTECH), *8(1),* 1-13.
https://doi.org/10.60093/jiciviltech.1899707
This work is licensed under CC BY 4.0

## 1. Introduction

Energy transmission lines are among the critical infrastructure systems that must remain operational after earthquakes. In particular, buried steel pipelines used for natural gas and oil transmission require a specialized seismic design approach because they extend over wide geographical areas and operate under operational conditions that demand uninterrupted service. During earthquakes, buried pipelines are primarily affected by two distinct mechanisms: transient ground deformations induced by seismic wave propagation and permanent ground deformation (PGD). Field observations and analytical studies have shown that a significant proportion of pipeline damage is caused by PGD effects and large fault-induced ground displacements (O'Rourke & Liu, 2012; Kennedy et al., 1977). While the effects of seismic wave propagation generally remain within elastic limits, fault crossings and ground discontinuities may impose substantial axial deformation and bending demands on pipelines (Liu et al., 2015).

The behavior of buried pipelines subjected to fault crossing was first modeled using the beam-on-elastic-foundation approach, in which pipe–soil interaction was idealized by Winkler-type springs (Newmark & Hall, 1982). This approach highlighted the decisive role of soil stiffness in governing pipeline response. Later, Takada et al. (2001) proposed simplified design formulations for fault crossing and introduced the concept of critical pipeline length. Karamanos and Dakoulas (2009), considering nonlinear material behavior, investigated the plastic deformation mechanisms of buried steel pipelines and demonstrated that soil stiffness and pipe wall thickness significantly influence deformation capacity. Vazouras et al. (2010) parametrically examined the effect of the D/t ratio on pipeline behavior under strike-slip fault crossings and showed that the risk of local buckling increases in thin-walled pipes. Similarly, Uçkan et al. (2015) evaluated the performance of buried steel pipelines under fault displacement using numerical models based on plastic hinge formation. These studies collectively indicate that pipeline behavior is highly sensitive to parameters such as fault displacement, soil stiffness, pipe diameter, and wall thickness.

In near-fault regions, high peak ground velocity (PGV) and long-period amplification are commonly observed due to forward directivity effects. Somerville (1997) demonstrated that near-fault effects can significantly increase deformation demands, particularly in flexible and extended structural systems. Because pipelines are linear and continuous systems, they are generally regarded as structures that are especially sensitive to ground velocity. Wang and Yeh (1985) showed that axial deformation demand is directly related to ground velocity. However, many studies in the literature have focused on deterministic fault rupture scenarios, whereas the direct integration of code-based near-fault coefficients into buried pipeline models through spectral analysis has been addressed only in a limited number of studies.

The Turkish Seismic Code for Pipeline Systems and Liquid Storage Tanks (TBHSDTDY, 2023) requires the application of both the maximum-direction factor and the near-fault factor in the determination of design spectral accelerations. This approach directly reflects the distance of the pipeline from active faults in the design parameters. However, comprehensive studies numerically demonstrating the effects of these code-defined coefficients on stress distributions and axial deformation demands in pipeline sections remain limited. Therefore, evaluating code-based spectral parameters together with finite element modeling is important for improving design safety.

In this study, the planned natural gas pipeline between Seydişehir in Konya Province and Ermenek in Karaman Province was considered as a case study. Although the route does not directly intersect an active fault zone, the Alacadağ Fault Zone is located approximately 9 km from the initial pigging station. According to the Turkish Earthquake Hazard Map, PGA values in the region range from 0.12g to 0.18g (AFAD, 2018). In accordance with the provisions of the code, the application of the near-fault factor results in an approximately 15–20% increase in design spectral accelerations. Numerical evaluation of the influence of this increase on the buried pipeline is therefore important from an engineering safety perspective.

Within the scope of this study, the design spectrum defined in the Turkish Seismic Code for Pipeline Systems and Liquid Storage Tanks was adopted, and the seismic behavior of the buried steel pipeline was investigated using the finite element method by considering the near-fault factor. The main objective of the study is to quantitatively determine the effect of the near-fault factor on displacement, stress, and axial deformation demands in the pipe section, and to assess the potential design bias that may arise if this factor is neglected.

The study is limited to linear-elastic spectral analysis, while permanent ground deformation (PGD), nonlinear material behavior, and deterministic fault rupture scenarios are excluded from its scope. In this respect, the study aims to contribute to the integration of a code-based design approach with numerical modeling.

## 2. Materials and Methods

### 2.1 Material Properties

The natural gas pipeline investigated in this study was manufactured from API 5L PSL2 Grade X46 steel. The pipe has an outer diameter of 273.1 mm and a wall thickness of 5.2 mm, resulting in a D/t ratio of approximately 52.5. The minimum yield strength, tensile strength, and modulus of elasticity of the steel were taken as 320 MPa, 435 MPa, and 210 GPa, respectively. Poisson's ratio was assumed to be 0.30. The pipe section exhibits the behavior of a thin-walled cylindrical shell. According to the PSL2 standard, since t/D (5.2/273.1 = 0.019) < 1/15, shell element modeling was preferred in SAP2000 v25.0, similar to the approach adopted by Raj et al. (2018). Although the material behavior was assumed to be elastic in the analyses, performance was assessed by comparing the obtained stress values with the yield strength. The potential for yielding was evaluated based on the von Mises equivalent stress criterion.

### 2.2 Ground Motion and Design Spectral Parameters

The ground motion was defined in accordance with the provisions of the Turkish Seismic Code for Pipeline Systems and Liquid Storage Tanks (2023). Article 2.3.5 of the code states that the maximum-direction effect, near-fault effect, and local site conditions shall be taken into account in determining the spectral parameters at the short period (0.2 s) and at the 1.0 s period. Within this framework, the mapped spectral acceleration at short period, *Ss*, and the mapped spectral acceleration at the 1.0 s period, $S_1$, for different earthquake ground motion levels were obtained from the Turkish Earthquake Hazard Maps (TDTH).
The spectral parameters were obtained from the AFAD Turkish Earthquake Hazard Map for the coordinates 37.419360° latitude and 32.053133° longitude. These coordinates were selected because, compared with the values obtained along the natural gas pipeline route, they correspond to a location closer to the active fault and yield more unfavorable spectral acceleration values. In the vicinity of the Seydişehir Pig Station, which is the starting point of the route, the Alacadağ Fault Zone is located approximately 9 km from the pipeline. Therefore, in accordance with the code provisions, consideration of the near-fault effect was deemed necessary. The earthquake ground motion parameters obtained from the TDTH are summarized in Table 1.

**Table 1.** Spectral acceleration values obtained from the AFAD Turkish Earthquake Hazard Map (TDTH)

| Earthquake Ground Motion Level | Ss (g) | S1 (g) | PGA (g) | PGV (cm/s) |
|---|---|---|---|---|
| **DD-1** | 0.709 | 0.172 | 0.316 | 14.639 |
| **DD-2** | 0.334 | 0.086 | 0.152 | 7.173 |
| **DD-3** | 0.120 | 0.033 | 0.055 | 2.733 |

For the DD-1a earthquake ground motion level, the PGA, PGV, S_s, and S_(1 )values were calculated using the logarithmic interpolation method. These calculations were performed using the following equations.

$$\log_{10}(PGVA_{D,DD\text{-}1a}) = 0.367 \log_{10}(PGA_{D,DD\text{-}1}) + 0.633 \log_{10}(PGA_{D,DD\text{-}2}) \quad (1)$$

$$\log_{10}(PGV_{D,DD\text{-}1a}) = 0.367 \log_{10}(PGV_{D,DD\text{-}1}) + 0.633 \log_{10}(PGV_{D,DD\text{-}2}) \quad (2)$$

$$\log_{10}(S_{s,DD\text{-}1a}) = 0.367 \log_{10}(S_{s,DD\text{-}1}) + 0.633 \log_{10}(S_{s,DD\text{-}2}) \quad (3)$$

$$\log_{10}(S_{1,DD\text{-}1a}) = 0.367 \log_{10}(S_{1,DD\text{-}1}) + 0.633 \log_{10}(S_{1,DD\text{-}2}) \quad (4)$$

The maximum-direction coefficients were taken as $\gamma_{PGA} = 1.1$ for PGA and $\gamma_{PGV} = 1.25$ for PGV, respectively. The coefficient representing the near-fault effect, $\phi_{1,\gamma F}$, was determined as 1.2, since the pipeline is located approximately 9 km from the fault. The distance relationship defined in the code is given below:

$$\varphi_{1,\gamma F} = 1.2\,, \quad (L_F \leq 15\ km) \quad (5)$$

The spectral acceleration values, considering the maximum-direction effect and the near-fault effect independently of site effects, were calculated using the following equations:

$$S_s' = \gamma_s\, S_s \quad (6)$$

$$S_1' = \gamma_1\, \varphi_{1,\gamma F}\, S_1 \quad (7)$$

In this study, $\gamma_s = 1.1$and $\gamma_1 = 1.3$were adopted. The calculated site-independent spectral parameters are presented in Table 2.

**Table 2.** Spectral parameters including the maximum-direction and near-fault effects.

| Earthquake Level | S's (g) | S'1 (g) | PGA' (g) | PGV' (cm/s) |
|---|---|---|---|---|
| **DD-1** | 0.780 | 0.268 | 0.348 | 21.959 |
| **DD-1a** | 0.484 | 0.173 | 0.219 | 13.980 |
| **DD-2** | 0.367 | 0.134 | 0.167 | 10.760 |
| **DD-3** | 0.132 | 0.051 | 0.061 | 4.100 |

The design spectral parameters, taking local site effects into account, were calculated as follows:

$$S_{DS} = F_s\, S_s' \quad (8)$$

$$S_{D1} = F_1\, S_1' \quad (9)$$

The local site effect coefficients were obtained from the relevant tables of the code and are presented in Table 3.

**Table 3.** Local site effect coefficients.

| Earthquake Level | Fs | F1 | FPGA | FPGV |
|---|---|---|---|---|
| **DD-1** | 1.200 | 1.500 | 1.300 | 1.300 |
| **DD-1a** | 1.300 | 1.500 | 1.300 | 1.300 |
| **DD-2** | 1.300 | 1.500 | 1.300 | 1.300 |
| **DD-3** | 1.300 | 1.500 | 1.300 | 1.300 |

The calculated site-dependent spectral parameters are summarized in Table 4.

**Table 4.** Site-dependent design spectral parameters.

| Earthquake Level | SDS (g) | SD1 (g) | PGAD (g) | PGVD (cm/s) |
|---|---|---|---|---|
| **DD-1** | 0.936 | 0.402 | 0.452 | 28.546 |
| **DD-1a** | 0.630 | 0.260 | 0.284 | 18.173 |
| **DD-2** | 0.478 | 0.201 | 0.217 | 13.987 |
| **DD-3** | 0.172 | 0.077 | 0.079 | 5.329 |

In this study, the site-dependent design spectral acceleration parameters determined in accordance with the provisions of the code were adopted in the finite element analyses. Accordingly, a realistic and safe seismic load definition was established by considering both the maximum-direction effect and the near-fault effect.

### 2.3 Finite Element Model

The finite element model was developed using SAP2000 V25 software. The pipeline was modeled as a continuous system with a total length of 13.5 m. This length was selected based on the observation that, in buried pipeline systems, deformations generally reach their maximum in the central region of the model, whereas stiffness increases toward the end regions due to soil restraint. Accordingly, the selected model length was intended to provide conservative estimates of the maximum stress and deformation demands that may occur at the critical section.

The pipe has an outer diameter of 273.1 mm and a wall thickness of 5.2 mm, resulting in a $D/t$ratio of approximately 52.5. For thin-walled cylindrical members ($D/t > 20$), section behavior is more accurately represented by shell theory. Since beam (frame) elements cannot adequately capture the circumferential and longitudinal stress distributions within the pipe wall, the model was established using four-node shell elements. This modeling approach allowed the hoop and longitudinal stress components to be obtained separately and enabled reliable calculation of the von Mises equivalent stresses. In the circumferential direction, 30° segments were used, resulting in 12 shell elements per cross-section. In the longitudinal direction, the element length was taken as 0.5 m. The mesh density was determined based on preliminary sensitivity analyses, and the adopted mesh corresponded to the point at which the stress and deformation results became effectively mesh-independent.

In buried pipeline systems, pipe–soil interaction is commonly represented using the elastic foundation approach. In this study, the soil was idealized by Winkler-type linear elastic springs. Based on the geotechnical data obtained from the project site, the modulus of subgrade reaction was taken as $K_s$=14000 kN/m$^3$. The equivalent spring stiffness corresponding to each shell element was calculated by considering the tributary contact area between the element and the surrounding soil, as given by

$$k_i = K_s \cdot A_i \quad (9)$$

where

- $k_i$= equivalent spring stiffness for the $i$-th node (kN/m)
- $K_s$= modulus of subgrade reaction $(\mathrm{kN/m^3})$
- $A_i$= tributary contact area associated with the corresponding shell element $(\mathrm{m^2})$

Since the shell elements were defined as 30° segments in the circumferential direction, the circumferential width of one element was approximately expressed as

$$b=R\cdot\Delta\theta \tag{10}$$

where $R = D/2$ is the pipe radius and $\Delta\theta$is the circumferential segment angle in radians. Accordingly, the contact area of one shell element was approximately calculated as

$$Ae=(R\cdot\Delta\theta)\cdot\Delta L \tag{11}$$

For interior nodes, the tributary area was approximately taken as $A_i \approx A_e/4$. With this approach, the spring stiffness values were distributed in a manner consistent with the mesh configuration of the shell model.

The spring stiffness values in the vertical and horizontal directions were calculated using the same modulus of subgrade reaction and were defined as

$$kv=Ks\cdot A(i) \tag{12}$$
$$kh=Ks\cdot Ai \tag{13}$$

No springs were assigned to the rotational degrees of freedom. In this way, the soil resistance against both vertical and horizontal displacements of the pipe was represented. The groundwater level was not considered in the analyses. This assumption was made because the site data indicated that the groundwater table was below the pipe burial depth.

Prior to the spectral analysis, a modal analysis was performed, and it was verified that the cumulative mass participation ratio of the first vibration modes exceeded 90%. This confirms that the dynamic behavior of the system was represented using a sufficient number of modes. Through this modeling approach, pipe–soil interaction was mathematically defined, and realistic stress distributions were obtained by means of shell elements.

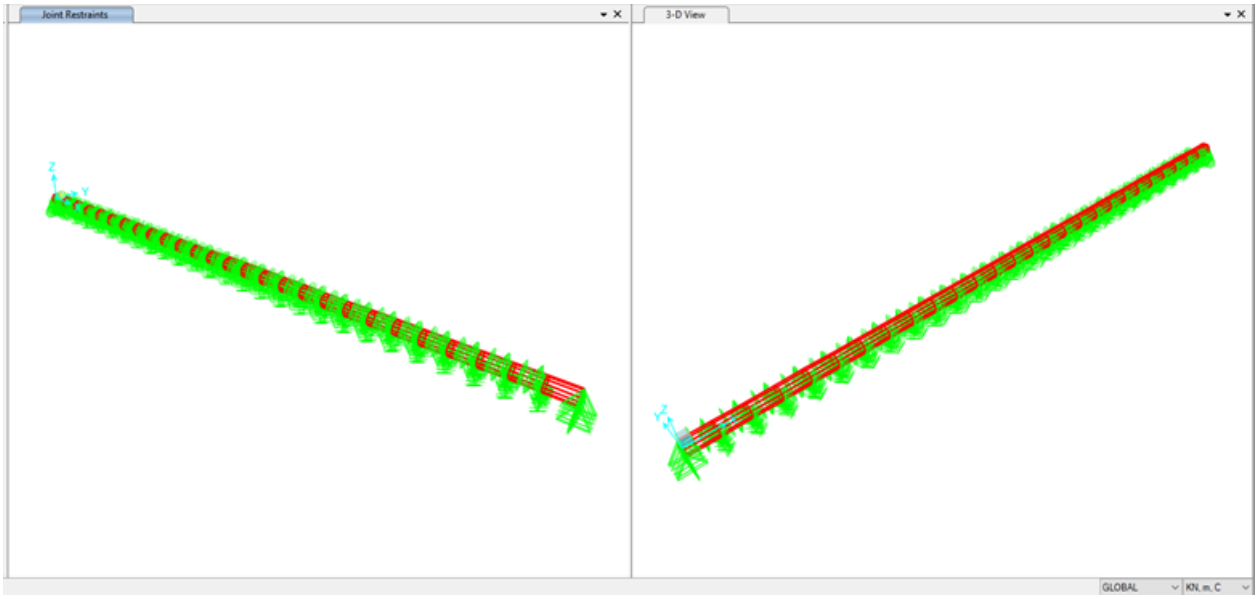



**Figure 1.** Assignment of spring stiffness values.

### 2.4 Loading Conditions

In the finite element model, both static and dynamic loading components were considered together in order to realistically represent the actual operating conditions of the pipeline. The self-weight of the pipe, backfill soil load, surface live load, and earthquake effect were defined in the model.

The self-weight of the pipe was automatically calculated by the software by considering the material density and cross-sectional geometry. The self-weight of the elements was assigned using the unit weight of steel. This load acts on the system as a uniformly distributed load.

The backfill soil load was applied to the model as an equivalent distributed load by considering the pipe burial depth and the unit weight of the soil. The vertical stress developed over the burial depth was calculated using the following equation:

$$\sigma_v = \gamma_s \cdot H \tag{14}$$

where:
$\gamma_s$= unit weight of the backfill soil (kN/m³),
$H$= soil cover thickness above the pipe (m)

The resulting vertical stress was applied to the outer surface of the pipe as an equivalent uniformly distributed load. The surface live load was idealized as an equivalent component transmitted to the pipe by considering the distribution of traffic-induced loads through the soil. This load was defined in the model as an equivalent static load, producing a decreasing effect in accordance with the principle of stress distribution within the soil.The earthquake load was applied through the response spectrum analysis method using the design spectrum determined in accordance with the provisions of the Turkish Seismic Code for Pipeline Systems and Liquid Storage Tanks (2023). Separate analyses were carried out for the DD-1, DD-1a, DD-2, and DD-3 earthquake ground motion levels. In the dynamic analysis, the SRSS method was adopted as the modal combination procedure.

In order to evaluate the effect of the near-fault coefficient on the structural response, two different spectral loading scenarios were considered. In the first scenario, the design spectrum including both the maximum-direction coefficient and the near-fault coefficient was used, whereas in the second scenario the near-fault coefficient was neglected. In this way, the variations in stress, displacement, and axial deformation demands were quantitatively compared.

Through this loading approach, both service loads and earthquake effects were evaluated together, and the performance of the pipeline under different earthquake levels was comprehensively analyzed.

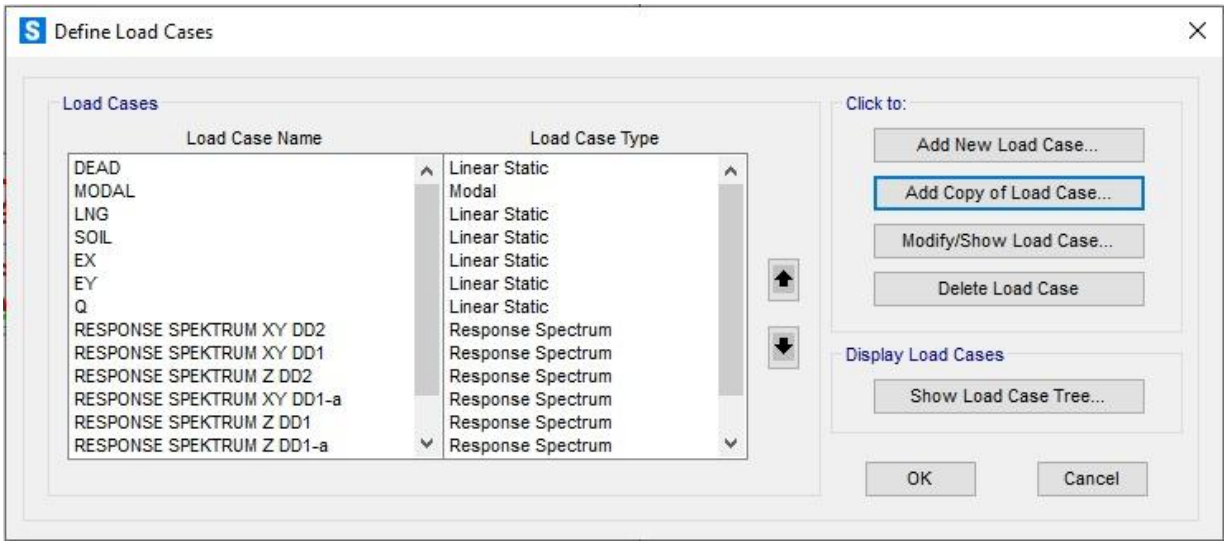



**Figure 2.** Definition of loading conditions.

**3. Results**

In this section, the displacement, stress, and strain results obtained from the finite element analyses are presented, and the effect of the near-fault coefficient on the structural response is evaluated. The analyses were performed for the DD-1, DD-2, and DD-3 earthquake ground motion levels, and the cases with and without the near-fault coefficient were comparatively examined.

### 3.1. Displacement Distributions

For the finite element model defined with a length of 13.5 m and a diameter of 10 in. (273.1 mm), the nodal displacement values obtained by considering the near-fault coefficient were examined for different earthquake ground motion levels. The analyses were carried out under the RESPONSE SPECTRUM DD-1 Z loading case.

At the DD-1 earthquake ground motion level, the maximum displacement was obtained as 10.42 mm in the U3 direction. In the same analysis, the maximum displacement in the U2 direction was approximately 0.32 mm, while the maximum displacement in the U1 direction was about 0.06 mm. These results indicate that the dominant deformation component of the system developed in the U3 direction.

Examination of the displacement contour diagram shows that the maximum displacement occurred in the middle region of the model. This can be explained by the increase in stiffness at the end regions due to the restraint provided by the soil springs in the buried pipeline model, which causes deformation to concentrate in the middle section. Owing to the pipe–soil interaction, the system exhibited a continuous elastic bending shape. The maximum displacement corresponds to approximately

$$\frac{10.42}{273.1} \times 100 \approx 3.8\% \tag{15}$$

of the pipe diameter. This ratio is not at a level indicating global instability or local shell buckling. The deformation distribution varied smoothly along the pipe axis, and no sudden concentration of deformation was observed. The application of the near-fault coefficient caused a noticeable increase in displacement demands compared with the previous analyses; however, the system remained within the elastic response limits at all earthquake levels. Figure 3 presents the displacement contour diagram of the nodal points for the DD-1 earthquake level.

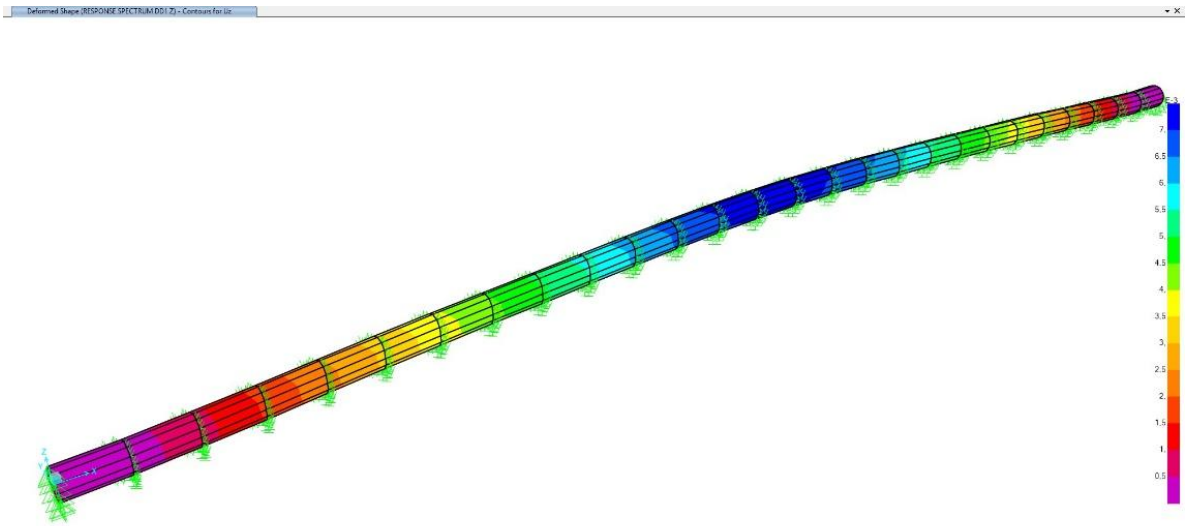


**Figure 3.** Vertical displacement contour of the buried steel pipeline at the DD-1 ground-motion level.

### 3.2 Stress Results

The stress distributions developed in the shell elements were examined based on the results of the Linear Response Spectrum analysis performed for the DD-1 earthquake ground motion level by considering the near-fault coefficient. Stress evaluations were carried out using the membrane stress components at the top surface of the shell elements ($S_{11}$, $S_{22}$, and $S_{12}$). According to the analysis results, the maximum axial membrane stress was obtained as 62.17 MPa in the $S_{11}$ direction. The maximum stress in the circumferential direction was found to be $S_{22} \approx 39.33$MPa, while the shear stress was determined as $S_{12} \approx 2.64$MPa. When the maximum axial stress is compared with the minimum yield strength of API 5L PSL2 Grade X46 steel, which is 320 MPa, the following ratio is obtained:

$$\frac{62.17}{320} \approx 0.19 \tag{16}$$

This value corresponds to approximately 19% of the yield stress. This result indicates that the pipe section remained within the elastic response range even under the most unfavorable DD-1 earthquake level in which the near-fault effect was taken into account. Examination of the stress contour diagrams shows that the maximum stress was concentrated in the middle region of the model. This observation is consistent with the displacement distribution and confirms that the system exhibited a continuous bending response. The stress distribution remained continuous along the pipe axis, and no sudden stress concentration indicating local shell buckling or yielding was observed. Although the application of the near-fault coefficient led to an increase in axial stress demands compared with the previous analyses, the stresses in the shell elements remained below the material capacity for all earthquake levels. Figure 4 presents the stress distribution in the shell elements for the DD-1 earthquake level.

The von Mises equivalent stress calculated from the shell element stress components was approximately 60–65 MPa, which corresponds to nearly 20% of the minimum yield strength of API 5L PSL2 Grade X46 steel. This result indicates that the system remained in the linear elastic range even at the DD-1 earthquake level when the near-fault effect was considered.

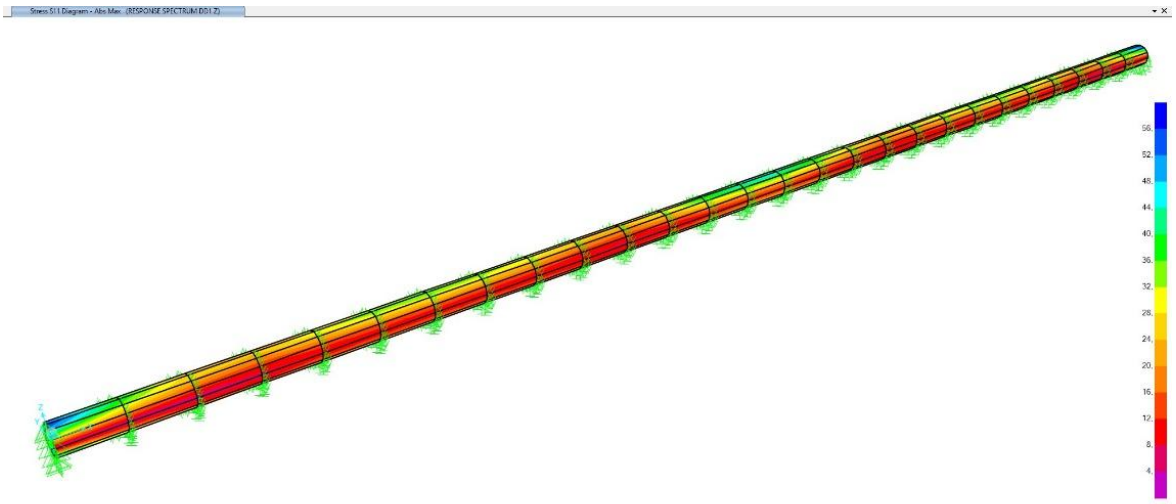


**Figure 4.** Stress distribution of the shell elements for the DD-1 earthquake level

### 3.3 Shear Stress Distributions

In the analysis results for the DD-1 earthquake ground motion level obtained by considering the near-fault coefficient, the membrane shear stresses ($S_{12}$)developed in the shell elements were examined. The maximum shear stress was obtained as:

$$\tau_{max} = S_{12,\max} \approx 9.21 \text{ MPa} \tag{17}$$

For API 5L PSL2 Grade X46 steel, taking the minimum yield strength as *fy= 320 MPa,* the approximate shear yield strength according to the von Mises criterion is calculated as

$$\tau_y \approx 0.577 f_y = 0.577 \times 320 \approx 185 \text{ MPa} \tag{18}$$

Accordingly, the ratio of the maximum shear stress to the shear yield strength is:

$$\frac{9.21}{185} \approx 0.05 \tag{19}$$

which corresponds to approximately 5%. This result indicates that, even at the DD-1 earthquake level where the near-fault effect was considered, the shear stresses remained well below the material capacity, and the system operated within the elastic range with respect to shear behavior.

Examination of the shear stress distribution shows that the maximum values were concentrated in the middle region of the model and were consistent with the bending response. No sudden increase in shear stress or local instability was observed along the pipe axis. Owing to the continuity provided by the soil springs, the stress distribution exhibited a balanced pattern. The shear stress values obtained for the DD-2 and DD-3 earthquake levels were lower than those

obtained for the DD-1 level. At all earthquake levels, the shear stresses in the shell elements remained well below the material capacity. Figure 5 presents shear stress distribution for the DD-1 earthquake level.

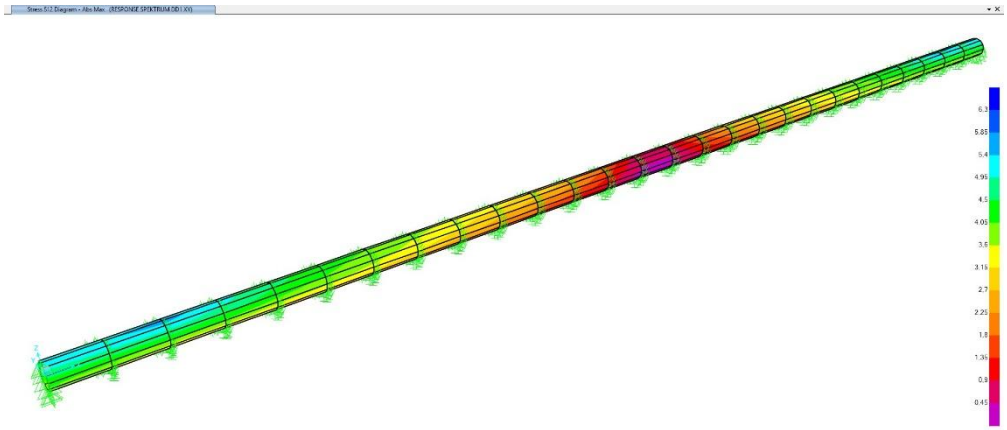


**Figure 5.** Shear stress (S_12 )distribution for the DD-1 earthquake level.

### 3.4 Axial Strain Results

The axial strains ($E_{11}$)developed in the shell elements were examined based on the results of the Linear Response Spectrum analysis performed for the DD-1 earthquake ground motion level by considering the near-fault coefficient. According to the analysis results, the maximum axial strain was obtained as $\varepsilon_{\max} = 0.000318$. Consistent with the displacement and stress results, the maximum strain values were concentrated in the middle region of the model.

For API 5L PSL2 Grade X46 steel, the yield strain is calculated from the following relationship:

$$\varepsilon_y = \frac{f_y}{E} \tag{20}$$

Taking $f_y$=320 MPa and $E$=210000 MPa, the yield strain is obtained as $\varepsilon_y \approx 0.00152$. Accordingly, the ratio of the maximum axial strain to the yield strain is

$$\frac{0.000318}{0.00152} \approx 0.21 \tag{21}$$

which corresponds to approximately 21%. This result indicates that, even under the most unfavorable DD-1 earthquake level in which the near-fault effect was taken into account, the pipe section did not reach the yielding limit, and the system remained within the elastic response range.

The strain distribution remained continuous along the pipe axis, and no sudden strain concentration or local behavior indicating shell instability was observed. Owing to the continuity provided by the soil springs, the system exhibited a stable bending pattern. Figure 6 presents the strain contour results of the shell elements.

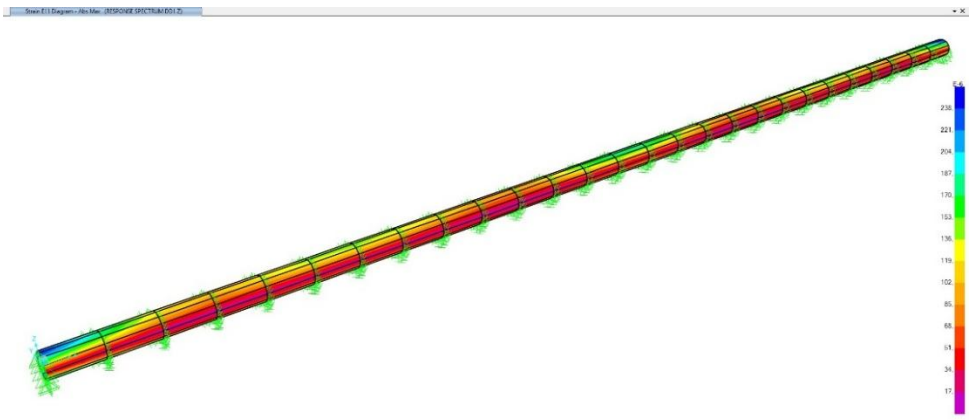


**Figure 6.** Strain distribution of the shell elements for the DD-1 earthquake level.

### 3.5 Internal Force Distributions

In the analyses performed for the DD-1 earthquake ground motion level by considering the near-fault coefficient, the membrane internal forces developed in the shell elements ($F_{11}$, $F_{22}$, and $F_{12}$) were examined. According to the analysis results, the maximum axial membrane force was obtained as $F_{11,\max} \approx 360.81$ N/mm. The maximum membrane force in the circumferential direction was determined as $F_{22,\max} \approx 224.3$ N/mm, while the shear membrane force was found to be $F_{12,\max} \approx 48$ N/mm. In shell elements, the membrane stress is calculated using the following relationship:

$$\sigma_{11} = \frac{F_{11}}{t} \tag{22}$$

where $t = 5.2$ mm is the pipe wall thickness. Accordingly, the maximum axial stress is calculated as

$$\sigma_{11,\max} = \frac{360.81}{5.2} \approx 69.4 \text{ MPa} \tag{23}$$

When this value is compared with the minimum yield strength of API 5L PSL2 Grade X46 steel, which is 320 MPa, the following ratio is obtained:

$$\frac{69.4}{320} \approx 0.22 \tag{24}$$

This corresponds to approximately 22% of the yield strength. This result indicates that the pipe section remained within the elastic response range even at the DD-1 earthquake level where the near-fault effect was considered.

Examination of the internal force distributions showed that the maximum axial membrane forces were concentrated in the middle section of the model. This observation is consistent with the displacement and stress distributions and confirms the continuous elastic bending response of the system. No sudden force concentration or local instability was observed along the pipe axis. Although the application of the near-fault coefficient led to an increase in membrane force demands, the resulting internal force values remained below the material capacity. Figure 7 presents the internal force contour results of the shell elements.

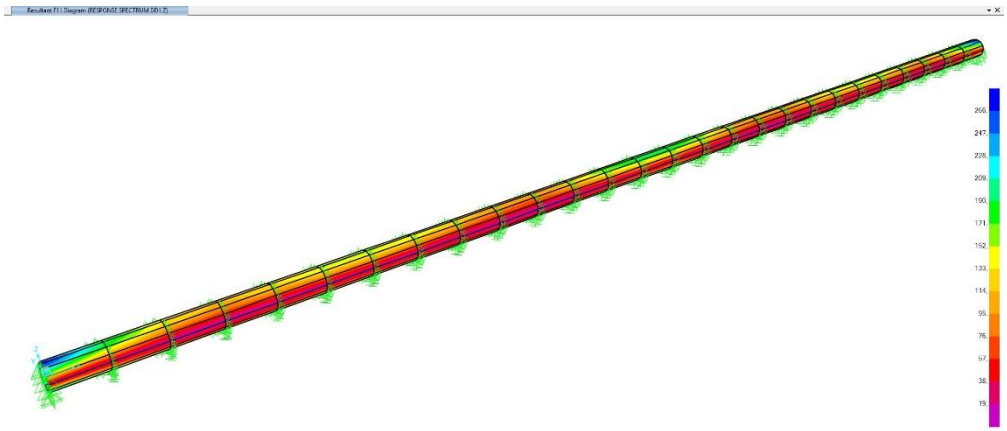


**Figure 7.** Internal force distribution for the DD-1 earthquake level.

### 3.6 Effect of the Near-Fault Coefficient on Seismic Demands

In this study, two different design spectra were used to quantitatively evaluate the effect of the near-fault coefficient on the seismic behavior of the buried steel pipeline:

- **NoNF (Without Near-Fault Effect):** The design spectrum was defined by considering only the maximum-direction coefficient.
- **NF (With Near-Fault Effect):** The design spectrum was established by considering both the maximum-direction coefficient and the near-fault coefficient.

Both analyses were carried out for the DD-1 earthquake ground motion level. The maximum displacement, membrane stresses ($S_{11}$), shear stresses ($S_{12}$), axial strain ($E_{11}$), and membrane internal

forces ($F_{11}$)obtained from the shell elements were compared. The percentage increase was calculated using the following equation:

$$\%Artış = \frac{T_{NF} - T_{NoNF}}{T_{NoNF}} \times 100 \tag{25}$$

where $T_{NF}$ represents the demand obtained by including the near-fault coefficient, and $\boldsymbol{T_{NoNF}}$represents the demand obtained without considering the near-fault coefficient.

**Table 5.** The Effect of the Near-Fault Coefficient on Structural Demands (DD-1).

| Demand Parameter | NoNF | NF | Increase (%) |
|---|---|---|---|
| Max. Displacement U3 (mm) | 7.364 | 10.419 | 41.5 |
| Max. Axial Stress S11 (MPa) | 56.53 | 62.81 | 11.1 |
| Max. Shear Stress S12 (MPa) | 7.30 | 9.21 | 26.0 |
| Max. Axial Strain E11 | 0.000245 | 0.000318 | 29.8 |
| Max. Membrane Force F11 (N/mm) | 278.11 | 360.81 | 29.7 |

The results indicate that the near-fault coefficient has a particularly pronounced effect on deformation-based demands. An increase of approximately 41% was observed in the maximum displacement, confirming that ground velocity amplification in near-fault regions significantly increases deformation demands in pipeline systems. In addition, increases of approximately 30% were observed in the membrane internal forces and axial strain values. In contrast, the increase in axial stress remained more limited, at approximately 11%. These findings demonstrate that neglecting the near-fault coefficient may lead to a significant underestimation, particularly of displacement and deformation demands.

## 4. Conclusions

In this study, the seismic response of a buried steel natural-gas pipeline subjected to code-based near-fault effects was evaluated through a spectrum-based finite element approach using the Seydişehir–Ermenek route as a case study. In accordance with the Turkish Seismic Code for Pipeline Systems and Liquid Storage Tanks (2023), the design spectra were established by incorporating both the maximum-direction factor and the near-fault factor, and their influence on the structural demands of the pipeline was quantitatively assessed.

The results showed that the near-fault factor has a pronounced influence particularly on deformation-based response quantities. At the DD-1 earthquake ground motion level, the maximum vertical displacement was obtained as 10.42 mm, which corresponds to approximately 3.81% of the pipe diameter. The maximum axial membrane stress was approximately 62 MPa, corresponding to nearly 19% of the minimum yield strength. The maximum axial strain was determined as 0.000318, which corresponds to approximately 21% of the yield strain. The maximum shear stress was 9.21 MPa, which is approximately 5% of the shear yield strength.

A comparative evaluation of the cases with and without the near-fault factor indicated that the inclusion of this coefficient increased the maximum vertical displacement by about 41%, while the axial strain and membrane force demands increased by nearly 30%. In contrast, the increase in axial stress remained relatively limited, at approximately 11%. These findings indicate that the near-fault factor affects not only the magnitude of the response but also the engineering interpretation of the governing demand type, making deformation-based assessment particularly important for buried pipeline systems located near active faults.

In all analysis scenarios, the system remained within the elastic response range, and no yielding or local shell instability was observed. Nevertheless, the results clearly demonstrate that neglecting the code-based near-fault factor may lead to unconservative estimates, especially in terms of displacement and deformation demands. From an engineering design perspective, such underestimation may affect the reliability of performance evaluations for buried steel pipelines in near-fault regions.

Therefore, it is recommended that the near-fault factor defined in the code should be explicitly incorporated into the spectrum-based design and assessment of buried steel pipelines located relatively close to active faults. The study also demonstrates that the integration of code-defined seismic coefficients with finite element modeling provides a practical and rational framework for evaluating the seismic safety of extended buried pipeline systems.

**Ethical Standards Statement**

The author declares that this study does not involve human or animal experiments and therefore does not require ethics committee approval. In addition, all ethical principles, including authorship, proper citation, data reporting, and the publication of original research, have been fully observed.

**Author Contributions Statement (CRediT)**

Author 1: Conceptualization, methodology/study design, software, formal analysis, investigation, resources, data curation, writing - original draft, writing - review and editing, visualization.

**Conflict of Interest Statement**

The author declares that there is no conflict of interest.

**Data Availability**

The data generated or analyzed during this study are presented within the article. Model inputs and additional computational outputs are available from the corresponding author upon reasonable request.

**Acknowledgments**

A short version of this study was presented as an abstract paper at the BILSEL Ahlat Congress.

**5. References**

AFAD (2018). Türkiye Deprem Tehlike Haritası ve Açıklama Raporu. Ankara.

American Lifelines Alliance (ALA). (2001). Guidelines for the design of buried steel pipe. FEMA.

American Petroleum Institute (API). (2018). Specification for Line Pipe (API 5L). Washington, DC.

Bray, J. D., & Travasarou, T. (2007). Simplified procedure for estimating earthquake-induced deviatoric slope displacements. Journal of Geotechnical and Geoenvironmental Engineering, 133(4), 381–392. doi:10.1061/(ASCE)1090-0241(2007)133:4(381)

Gresnigt, A. M. (1986). Plastic design of buried steel pipelines in settlement areas. Heron Journal, 31(4).

Honegger, D. G., & Nyman, D. J. (2004). Guidelines for the seismic design of oil and gas pipeline systems. Proceedings of IPC2004. doi:10.1115/IPC2004-0252

Karamanos, S. A., & Dakoulas, P. (2009). Mechanical behavior of buried pipes crossing active faults. Journal of Geotechnical and Geoenvironmental Engineering, 135(6), 821–834. doi:10.1061/(ASCE)GT.1943-5606.0000035

Kennedy, R. P., Chow, A. W., & Williamson, R. A. (1977). Fault movement effects on buried oil pipeline. Transportation Engineering Journal, 103(5), 617–633. doi:10.1061/TPEJAN.0000893

Liu, A., O'Rourke, M. J., & Zhang, J. (2015). Effects of permanent ground deformation on buried steel pipelines. Soil Dynamics and Earthquake Engineering, 76, 140–152. doi:10.1016/j.soildyn.2015.04.002

Newmark, N. M., & Hall, W. J. (1982). Earthquake spectra and design. Earthquake Engineering Research Institute. doi:10.1193/1.1585808

O'Rourke, M. J., & Liu, X. (2012). Seismic design of buried and offshore pipelines. MCEER Monograph. doi:10.1007/978-1-4614-0140-2

Somerville, P. G. (1997). Characterizing near-fault ground motion. Earthquake Spectra, 13(1), 123–153. doi:10.1193/1.1585892

Takada, S., Hassani, N., & Fukuda, K. (2001). A new proposal for simplified design of buried steel pipes crossing active faults. Earthquake Engineering & Structural Dynamics, 30(8), 1243–1257. doi:10.1002/eqe.57

Türkiye Boru Hatları ile Petrol Taşıma A.Ş. (2023). Türkiye Boru Hattı Sistemleri ve Sıvı Depolama Tankları Deprem Yönetmeliği. Ankara.

Uckan, E., O'Rourke, M., & Gresnigt, A. (2015). Behavior of buried steel pipelines subjected to strike-slip faulting. Journal of Pressure Vessel Technology, 137(3), 031701. doi:10.1115/1.4029552

Vazouras, P., Karamanos, S. A., & Dakoulas, P. (2010). Mechanical behavior of buried steel pipes crossing active strike-slip faults. Soil Dynamics and Earthquake Engineering, 30(11), 1361–1376. doi:10.1016/j.soildyn.2010.06.011

Wang, L. R. L., & Yeh, Y. H. (1985). A refined seismic analysis and design of buried pipelines for fault movement. Earthquake Engineering & Structural Dynamics, 13(1), 75–96. doi:10.1002/eqe.4290130107